Int. J. Heat Mass Transfer. Vol. 36, No. 15, pp. 3677–3686, 1993
Printed in Great Britain

0017–9310/93 $6.00+0.00
© 1993 Pergamon Press Ltd

The optimal cooling of a stack of heat generating boards with fixed pressure drop, flowrate or pumping power

STEFANO MEREU,† ENRICO SCIUBBA† and ADRIAN BEJAN‡

† Department of Mechanical and Aeronautical Engineering, University of Rome 1, 'La Sapienza', Rome, Italy and ‡ Department of Mechanical Engineering and Materials Science, Duke University, Durham, NC 27706, U.S.A.

(*Received* 8 *February* 1993 *and in final form* 1 *April* 1993)

Abstract—In this paper, we show analytically how to optimize the spacing between heat generating boards in a stack cooled by single-phase laminar forced convection. The thickness of each board is not negligible. The theoretical results for optimal spacing and maximum overall thermal conductance between stack and coolant are validated by means of numerical simulations of the complete flow and temperature fields. Results are reported for three different situations, which are dictated by the way in which the stack is attached to the rest of the cooling network of the electronics package: (1) fixed pressure drop, (2) fixed mass flowrate, and (3) fixed pumping power.

1. INTRODUCTION

To DETERMINE the optimal spacing of parallel heat generating plates in a stack of finite extent is a fundamental problem in the design of finned heat exchanger surfaces and packages of electronics. In both cases, the problem is analogous to determining the geometry in which the heat transfer rate extracted from the entire stack is maximum.

Recent reviews [1, 2] show that this problem has received considerable coverage in the electronics cooling literature; however, the published work refers to cooling by natural convection. For example, Bejan [3] and Bar-Cohen and Rohsenow [4] showed that the optimal spacing corresponds to a channel flow of the entrance type, in which the thermal boundary layers just touch at the downstream end of the channel. This problem was considered earlier by Elenbaas [5] and Levy [6]. More recently, the natural convection problem was solved in more general terms numerically by Kim *et al.* [7] and Anand *et al.* [8, 9], who considered the interaction between adjacent channels and the effect of asymmetry between the thermal boundary conditions specified on the two sides of one channel.

Although considerable work has been devoted also to channels cooled by forced convection (see, for example, refs. [1–3, 10 and 11]), the optimal spacing had not been recognized as an opportunity for maximizing the heat transfer, because in these studies the coolant flowrate was fixed. Recent work on micro-channel integrated heat sinks [12, 13] showed that when the imposed pressure difference across the channels is fixed, there exists an optimal fin-to-fin spacing for maximum total heat transfer rate. Bejan and Sciubba [14] showed that a similar optimum occurs in the design of a stack of smooth and negligibly thin heat generating boards.

The first objective of this paper is to develop optimal spacing results for stacks that reproduce more closely the features encountered in actual electronic packages. For example, the finite thickness of each board is taken into account in the calculation of the optimal board-to-board spacing and maximum heat transfer rate from the stack. Results are developed for three flow configurations (stacks with fixed pressure drop, fixed flowrate, or fixed pumping power), depending on how the stack is attached to the coolant network of the package of electronics. The second objective is to validate these optimal results based on complete simulations of the flow and temperature fields in the vicinity of each board.

2. OPTIMAL GEOMETRY OF PACKAGES WITH FIXED PRESSURE DROP

We begin with a generalization of the analysis of ref. [14], by including this time the effect of the board thickness t (Fig. 1). This effect was neglected in ref. [14], where it was assumed that t is always much smaller than D. This generalization of the analysis serves the additional purpose of redefining the terminology and basis for the existence of an optimal stacking of the boards in a given space (thickness H, and length L). If we assume that the number of boards in the stack is large, that number is

$$n = \frac{H}{D+t}. \quad (1)$$

(a) In the limit of sufficiently narrow channels ($D/L \to 0$), the mean velocity through each channel is the same as in Poiseuille flow

NOMENCLATURE

B_1 dimensionless conductance for constant pressure drop, equation (25)
$B_{1,peak}$ B_1 value corresponding to $D = D_{opt}$
B_2 dimensionless conductance for constant flowrate, equation (34)
B_3 dimensionless conductance for constant pumping power, equation (48)
$B_{3,peak}$ B_3 value corresponding to $D = D_{opt}$
c_P specific heat at constant pressure [kJ (kg·K)$^{-1}$]
C_1, C_2 constants
D board-to-board spacing [m], Fig. 1
D_c critical spacing [m], equation (33)
H overall thickness of stack [m], Fig. 1
k thermal conductivity [W (m·K)$^{-1}$]
L length of board [m], Fig. 1
L_d downstream length [m], Fig. 2
L_u upstream length [m], Fig. 2
$\dot{m}'$ mass flowrate [kg (s·m)$^{-1}$]
M dimensionless flowrate, equation (36)
n number of boards in the stack
p dimensionless pressure, equation (18)
P pressure [N m^{-2}]
$\mathbf{P}$ pumping power [W m^{-1}]
ΔP pressure difference [N m^{-2}]
Pr Prandtl number, ν/α
Re Reynolds number, equation (19)
q' total heat transfer rate [W m^{-1}]
q'_1 heat transfer rate from one surface [W m^{-1}], equation (6)
q'' heat flux [W m^{-2}]
t board thickness [m], Fig. 1
T temperature [K]
T_w surface temperature [K]
T_∞ inlet temperature [K]
u, w dimensionless velocity components, equation (17)
U, W velocity components [m s^{-1}], Fig. 2
$\bar{U}$ mean channel velocity [m s^{-1}], equation (2)
U_∞ free stream channel velocity [m s^{-1}]
U_0 inlet velocity [m s^{-1}], Fig. 2
x, z dimensionless coordinates, equation (17)
X, Z coordinates [m], Fig. 2.

Greek symbols
α thermal diffusivity [m^2 s^{-1}]
θ dimensionless temperature, equation (18)
μ viscosity [kg (s·m)$^{-1}$]
ν kinematic viscosity [m^2 s^{-1}]
Π dimensionless pressure difference, equation (9)
ρ density [kg m^{-3}]
Φ dimensionless pumping power, equation (47).

Subscripts
$(\ )_a$ Poiseuille flow limit
$(\ )_b$ boundary layer flow limit
$(\ )_{max}$ maximum
$(\ )_{opt}$ optimum.

Fig. 1. Two-dimensional space filled with a stack of heat generating boards cooled by forced convection.

$$U = \frac{D^2}{12\mu}\frac{\Delta P}{L} \tag{2}$$

where ΔP is the pressure difference maintained across the stack. We are assuming that the surfaces are smooth, and the contraction and enlargement effects are negligible. The mass flowrate per unit length normal to the stack profile $H \times L$ is $\dot{m}' = \rho U D n$, which means that

$$\dot{m}' = \frac{\rho H D^2}{12\mu(1+t/D)}\frac{\Delta P}{L}. \tag{3}$$

In the same limit, the outlet temperature of the coolant matches the temperature of the trailing edge of the board. We assume for simplicity that the board surface is isothermal at T_w, which means that the total rate of heat transfer removed from the stack is $q'_a = \dot{m}' c_P (T_w - T_\infty)$, where T_∞ is the coolant inlet temperature. By using equation (3), we conclude that

$$q'_a = \frac{\rho H D^2}{12\mu(1+t/D)}\frac{\Delta P}{L} c_P (T_w - T_\infty). \tag{4}$$

It is important to note that in the scale analysis presented in this section, the assumption that the board is isothermal at T_w means that we regard T_w as the scale of the surface temperature, i.e. a scale that is *distinct* from (and greater than) the coolant initial temperature T_∞. This assumption is not meant to imply in any way that the board substrate is a perfect thermal conductor. On the contrary, in the numerical simulation of the complete flow and temperature fields (Sections 3–6) we modelled the board surfaces as surfaces with uniform heat flux, which is a very good model for boards carrying flush mounted electronics.

It is worth noting also that in the earlier study of the stack with boards with negligible thickness [14], the type of scale analysis shown in this section was performed in two ways. In the first version, the board surface temperature was assumed uniform, while in the second the board surface was modelled as uniform flux. The order of magnitude results (e.g. optimal board to board spacing) produced by the two analyses were identical. This means that in the present scale analysis the board temperature T_w assumed above, equation (4), plays the same role as the L-averaged surface temperature when the board surface is modelled as uniform flux. This point will be tested numerically in Section 4, and discussed under equation (27).

(b) In the opposite limit, the board to board spacing D becomes large enough so that each surface is lined by a distinct laminar boundary layer. The fluid velocity through the channel, U_∞, is obtained by combining the longitudinal force balance $\Delta P \cdot D = 2L\tau_w$ with the Blasius solution for the L-averaged skin friction, $\bar{\tau}_w = 0.664\rho U_\infty^2 (U_\infty L/\nu)^{-1/2}$. The result is

$$U_\infty = \left(\frac{\Delta P D}{1.328 \rho L^{1/2} \nu^{1/2}}\right)^{2/3}. \tag{5}$$

According to the Pohlhausen solution for the same boundary layer flow, the heat transfer rate released by one surface is

$$q'_1 = 0.664 k (T_w - T_\infty) Pr^{1/3} \left(\frac{U_\infty L}{\nu}\right)^{1/2}. \tag{6}$$

This means that the entire stack releases $q'_b = 2nq'_1$, in other words

$$q'_b = 1.208 k H \frac{T_w - T_\infty}{1+t/D}\left(\frac{Pr L \Delta P}{\rho \nu^2 D^2}\right)^{1/3}. \tag{7}$$

The two asymptotes of the $q'(D)$ function, equations (4) and (7), show that q' increases roughly as D^2 when D is small, and decreases as $D^{-2/3}$ when D is large. There is a q' maximum at an intermediate channel spacing, D_{opt}: the order of magnitude of this optimal spacing is the same as the D obtained by intersecting the asymptotes, $q'_a \cong q'_b$. The result is

$$\frac{D_{opt}}{L} \cong 2.73 \Pi^{-1/4} \tag{8}$$

where Π is the dimensionless number associated with the imposed pressure difference [14, 15],

$$\Pi = \frac{\Delta P L^2}{\mu \alpha}. \tag{9}$$

The corresponding maximum heat transfer rate released from the H-thick package is obtained by substituting $D \cong D_{opt}$ in equation (4) or equation (7)

$$q'_{max} \lesssim 0.62 \frac{H c_P (T_w - T_\infty)}{1+t/D_{opt}}\left(\frac{\rho \Delta P}{Pr}\right)^{1/2}. \tag{10}$$

If the analysis of equations (1)–(10) is repeated for a stack in which each board has one surface heated (T_w) and the other insulated, the corresponding results for optimal spacing and maximum total heat transfer rate are

$$\frac{D_{opt}}{L} \cong 2.10 \Pi^{-1/4} \tag{11}$$

$$q'_{max} \lesssim 0.37 \frac{H c_P (T_w - T_\infty)}{1+t/D_{opt}}\left(\frac{\rho \Delta P}{Pr}\right)^{1/2}. \tag{12}$$

The inequality sign used in equations (10) and (12) is a reminder that the maximum of the actual $q'(D)$ curve is located *under* the point of intersection of the q'_a and q'_b asymptotes. The order of magnitude of the maximum q' value is represented well by the right-hand side of equation (10), or equation (12).

A new result shown by equations (8) and (11) is that the board thickness t has no effect on the optimal channel spacing. The latter depends on the imposed pressure difference, the flow length L, and the coolant properties. Another new result is that a non-negligible board thickness will have an effect on the maximum heat transfer rate. Equations (10) and (12) show that q'_{max} decreases when t increases and becomes comparable with the board-to-board spacing. These theor-

etical predictions will be validated by the numerical experiments described in Section 4.

3. MATHEMATICAL FORMULATION AND NUMERICAL METHOD

The effect of the board-to-board spacing on the total heat transfer rate q' (or the rate of heat generation in the $H \times L$ space) was studied numerically. The flow and heat transfer were simulated in an elementary control volume that contains only one board (Fig. 2). The control volume has a thickness $D+t$, and a total length $L_u + L + L_d$, where L_u and L_d are the lengths of the computational domain situated upstream and, respectively, downstream of the board. The chosen ratios L_u/L and L_d/L are large enough (namely, $L_u/L = 0.6$, $L_d/L = 1$, for this entire study) so that the flow field around the board is not sensitive to further increases in their values. The inlet velocity U_0 and temperature T_∞ are assumed uniform in the plane $X = 0$.

It is assumed that the boards are sufficiently wide in the direction perpendicular to the plane of Fig. 2 such that the flow is essentially two-dimensional in the x–z plane. The nondimensional equations that govern the conservation of mass, momentum and energy in the fluid portions of the control volume are

$$\frac{\partial u}{\partial x} + \frac{\partial w}{\partial z} = 0 \quad (13)$$

$$u\frac{\partial u}{\partial x} + w\frac{\partial u}{\partial z} = -\frac{\partial p}{\partial x} + \frac{1}{Re}\nabla^2 u \quad (14)$$

$$u\frac{\partial w}{\partial x} + w\frac{\partial w}{\partial z} = -\frac{\partial p}{\partial z} + \frac{1}{Re}\nabla^2 w \quad (15)$$

$$u\frac{\partial \theta}{\partial x} + w\frac{\partial \theta}{\partial z} = \frac{1}{Re\,Pr}\nabla^2 \theta \quad (16)$$

where $\nabla^2 = \partial^2/\partial x^2 + \partial^2/\partial z^2$, and the nondimensional variables are indicated by lower case letters

$$(x, z) = \frac{(X, Z)}{L}, \quad (u, w) = \frac{(U, W)}{U_0} \quad (17)$$

$$p = \frac{P}{\rho U_0^2}, \quad \theta = \frac{T - T_\infty}{q'' L/k} \quad (18)$$

$$Re = \frac{U_0 L}{\nu}, \quad Pr = \frac{\nu}{\alpha}. \quad (19)$$

The board surfaces are smooth, impermeable, and with no slip ($u = w = 0$). The upper surface releases the uniform heat flux q''

$$\frac{\partial \theta}{\partial z} = -1, \quad \text{at} \quad \frac{L_u}{L} < x < \frac{L_u}{L} + 1 \quad \text{and} \quad z = \frac{t/2}{L} \quad (20)$$

while the remaining three surfaces are adiabatic. The boundary conditions on the outer perimeter of the control volume are

$$u = 1, \quad w = \theta = 0, \quad \text{at} \quad x = 0 \quad (21)$$

$$\frac{\partial}{\partial x}(u, w, \theta) = 0 \quad \text{at} \quad x = (L_u + L + L_0)/L \quad (22)$$

$$w = 0 \quad \text{at} \quad z = \pm(D+t)/2L \quad (23)$$

$$(u, \theta)_{z = +(D+t)/2L} = (u, \theta)_{z = -(D+t)/2L}. \quad (24)$$

The boundary conditions (23) reflect the assumption that the Reynolds number Re is small enough so that the flow is laminar and symmetric about the board

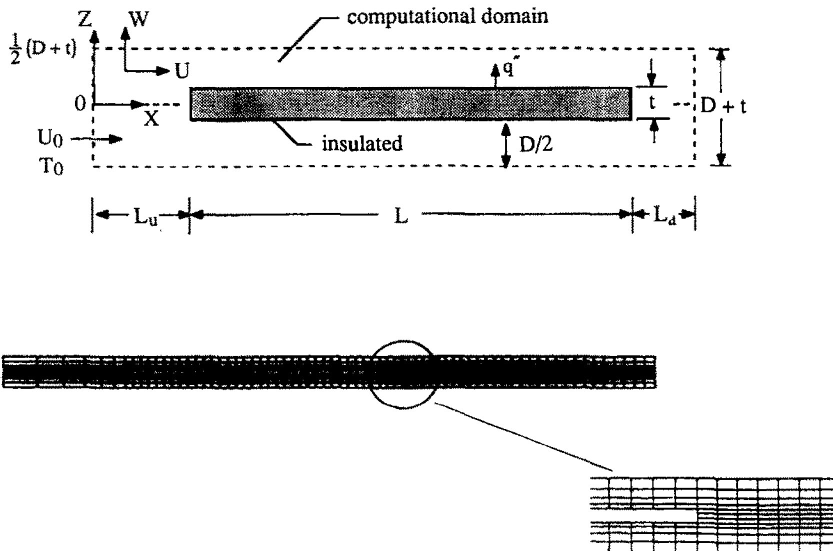

FIG. 2. The computational domain, thermal boundary conditions on the board surfaces, and the non-uniform grid used for the case $Re = 1000$, $D/L = 0.1$, $t/L = 0.02$, $L_u/L = 0.6$ and $L_d/L = 1$.

midplane. It is worth noting that if this study were to be extended to boards covered with protruding heat sources (blocks), recirculation may occur between the plates, and the flow symmetry condition (23) is no longer appropriate. In such cases, the w condition (23) must be replaced by a w continuity condition of type (24).

Note further that the repeated boundary condition (24) means that the numerical simulation based on Fig. 2 refers to one of the internal boards of the stack shown in Fig. 1. The top and bottom channels sketched in Fig. 1 differ from the half-channels of Fig. 2 only with respect to one flow boundary condition. In Fig. 1, the top and bottom planes (the plates that confine the stack) are adiabatic, impermeable and no slip. In Fig. 2, the plane of symmetry $z = (D+t)/2L$ is adiabatic, impermeable and zero-shear. In the design optimization work that follows, it is assumed that the total number of boards n is of the order of 10 or greater, so that the overall performance of the stack of Fig. 1 is essentially the same as that of a stack of n control volumes of the type shown in Fig. 2.

The forced convection heat transfer problem stated in equations (13)–(24) was solved for $u(x, z)$, $w(x, z)$ and $\theta(x, z)$ using the commercial finite-element package FIDAP [16]. The first objective of these calculations was to determine the point of the board surface with the highest temperature, T_{max}, or dimensionless, $\theta_{max} = (T_{max} - T_\infty)/(q''L/k)$. The overall thermal conductance of the package, $q'/(T_{max} - T_\infty)$, was then minimized while varying the geometric parameters of the $H \times L$ package of heat generating boards. The optimization procedure and its results are described in Sections 4–6.

Special care was taken to select a nonuniform grid that is fine enough so that the calculated values of the maximum surface temperature (θ_{max}) and the end-to-end pressure drop ($\Delta p = \bar{p}(0) - \bar{p}(L_u/L + 1 + L_d/L)$, where $\bar{p}$ represents an average in the z direction) are sufficiently insensitive to further grid refinements. The grid selected for the case $Re = 1000$, $D/L = 0.1$, $t/L = 0.02$, $L_u/L = 0.6$, and $L_d/L = 1$, is illustrated in the lower half of Fig. 2. This grid, which has a total of 671 elements, was chosen based on accuracy tests of the type illustrated here in Table 1. The elements employed in the simulation were isoparametric, 9-nodes quadrilateral, with linear pressure approximation.

Table 1. Accuracy test: the effect of grid fineness on the numerical solution for maximum temperature and overall pressure drop ($Re = 1000$, $D/L = 0.1$, $t/L = 0.02$, $L_u/L = 0.6$, $L_d/L = 1$)

Elements	Nodes	θ_{max}	Δp
119	574	0.94	1.86
274	1242	0.94	1.84
424	1872	0.93	1.83
671	2918	0.93	1.80
1096	4676	0.93	1.80

4. THE OVERALL THERMAL CONDUCTANCE OF THE PACKAGE

The total rate of heat generation due to n boards in the $H \times L$ stack of Fig. 2 is $q' = nq''L$. The objective is to maximize q' while keeping T_{max} below a certain (safe) level, or to maximize the overall thermal conductance defined as the ratio $q'/(T_{max} - T_\infty)$. It is convenient to nondimensionalize the overall conductance by using the q'_{max} scale derived in equations (10) and (12)

$$B_1 = \frac{q'/(T_{max} - T_\infty)}{Hc_P(\rho \Delta P/Pr)^{1/2}}. \tag{25}$$

This definition can be rewritten using the θ_{max} and Π definitions, equations (18) and (9)

$$B_1 = \left[\left(\frac{D}{L} + \frac{t}{L}\right)\theta_{max}\Pi^{1/2}\right]^{-1} \tag{26}$$

to show that the objective function B_1 depends on the imposed pressure difference (Π), channel spacing (D/L), and, through θ_{max} on two additional parameters (t/L, Pr).

Figures 3(a)–(c) show that the overall thermal conductance B_1 is maximum when the board-to-board spacing reaches an optimal value. All the information plotted in Fig. 3 (and, later, in Figs. 4 and 5) was obtained numerically. The actual numerical data are indicated by larger symbols, while the curves have been added to visualize the trend of each group of data. The three frames of Fig. 3 were drawn for different values of the pressure drop number Π, namely, 9×10^5, 1.5×10^6 and 2.1×10^6. If in the reference case considered in Table 1 the fluid is air, these Π values correspond to the Re values 500, 750 and, respectively, 1000. The use of the $(D/L)\Pi^{1/4}$ group on the abscissa was suggested by equation (11): the numerical results presented in Fig. 3 validate equations (8) and (11), and, in particular, the prediction that the board thickness (t/L) does not influence the optimal board-to-board spacing. The best fit for the nine D_{opt} cases documented in Figs. 3(a)–(c) is

$$\frac{D_{opt}}{L}\Pi^{1/4} \cong 2.8. \tag{27}$$

Although in an order of magnitude sense equations (8), (11) and (27) are essentially the same, it is worth noting that the analytical formula derived for the model with both surfaces isothermal, equation (8), yields almost the same values for D_{opt} as the correlation of the present numerical results, equation (27).

The peak value of the overall thermal conductance, $B_{1,peak}$, depends on the board thickness t/L and the pressure drop number Π. The numerical results of Fig. 3 can be correlated by noting that equation (12) can be rewritten in view of equation (25)

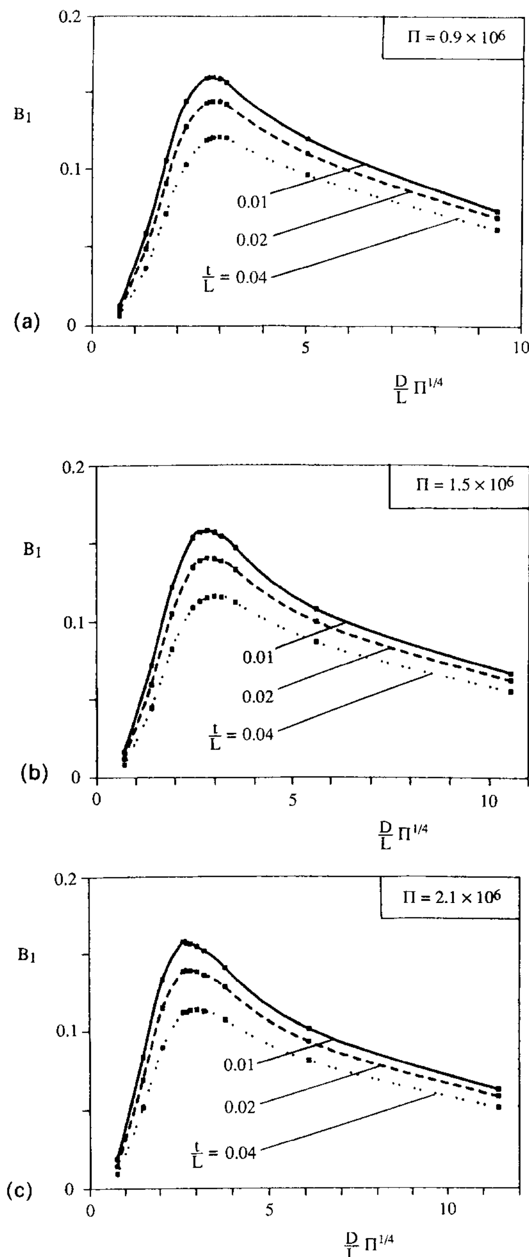

FIG. 3. The maximization of the overall thermal conductance at fixed pressure difference: the effect of the board thickness ($Pr = 0.7$).

$$B_{1,\text{peak}} \leqslant \frac{0.37}{1+\dfrac{1}{C_1}\dfrac{t}{L}\Pi^{1/4}} \tag{28}$$

in which $C_1 = 2.8$ is the constant found in the correlation of equation (27). The numerical $B_{1,\text{peak}}$ data of Fig. 3 are correlated within 5% by a similar expression

$$B_{1,\text{peak}} \cong \frac{0.18}{1+\dfrac{1}{2.8}\dfrac{t}{L}\Pi^{1/4}}. \tag{29}$$

This correlation proves the validity of the scaling law and the direction of the inequality sign that appear in equation (12).

5. OPTIMAL GEOMETRY OF PACKAGES WITH FIXED MASS FLOWRATE

The optimal board-to-board spacings determined in Sections 2 and 4 refer to a package with prescribed pressure difference, ΔP. The fixed-ΔP assumption is a good model for installations in which several parallel packages and other components (e.g. channels) receive their coolant from the same plenum. The plenum pressure is maintained by a fan or, in the case of a liquid coolant, by a pump. The fan or pump may be located upstream or downstream of the packages that are being cooled by forced convection.

The constant-ΔP model is not appropriate in a flow arrangement in which the H-thick package of interest is placed in series with other components (flow passages) that have a considerably larger flow resistance than the package itself. In such an application, the pressure difference that is maintained by the fan or pump is spent mainly on the components with the dominant flow resistance. From the point of view of the H-thick package that must be optimized, the effect of the more resistive portion of the flow circuit is to fix the mass flowrate through the package. In this section, we extend the geometric optimization method of Section 2 to a package with prescribed mass flowrate $\dot{m}'$.

(a) The limit $D/L \rightarrow 0$ is characterized by an outlet coolant temperature that approaches the board temperature T_w, which is assumed uniform. The total rate of heat transfer removed from the package is

$$q'_a = \dot{m}' c_P (T_w - T_0). \tag{30}$$

Important to note is that in this limit the rate of heat removal is independent of both the individual channel spacing (D) and board thickness (t).

(b) When D/L is large enough so that each board is sandwiched between distinct boundary layers, the heat transfer rate from one surface is described by the q'_1 expression listed in equation (6). The free stream velocity U_∞ is dictated by the fixed flowrate and the package geometry, $U_\infty = \dot{m}'/\rho n D$, or

$$U_\infty = \frac{\dot{m}'}{\rho H}\left(1+\frac{t}{D}\right). \tag{31}$$

The total heat transfer rate removed from the package is $q'_b = 2nq'_1$, or, after using the q'_1 expression and equation (31)

$$q'_b = 1.328k(T_w - T_\infty)Pr^{1/3}\left[\frac{\dot{m}' HL}{\mu D(D+t)}\right]^{1/2}. \tag{32}$$

The important feature of the large-D asymptote, equation (32), is that the total heat transfer rate removed from the package decreases roughly as $1/D$ as D increases. Combined with the behavior of q' in the opposite limit, equation (30), this means that the

maximum heat transfer rate is reached on the plateau represented by equation (30), provided the spacing D is small enough. The critical board-to-board spacing D_c, which distinguishes q'_a (or $D \ll D_c$) from q'_b (or $D \gg D_c$) is obtained by intersecting the $q'(D)$ curves (30) and (32)

$$\frac{D_c}{L}\left(1+\frac{t}{D_c}\right) \cong 1.328\,Pr^{-2/3}\left(\frac{\mu H}{\dot{m}'L}\right)^{1/2}. \quad (33)$$

Equation (33) shows that when the flowrate $\dot{m}'$ increases and the t/D ratio is of the order of 1 or smaller, the critical spacing D_c decreases approximately as $(\dot{m}')^{-1/2}$. Worth noting is that the dimensionless group $\dot{m}'L/\mu H$ is of the same order of magnitude as the Reynolds number based on length, UL/ν, where U is the mean velocity in the D channel.

The maximum rate of heat removal is achieved as soon as the order of D becomes smaller than the order of D_c: then, the maximum q' approaches the q'_a value calculated based on equation (30). Said another way, no additional benefit is derived from decreasing D further (i.e. adding more boards in the H-thick space), if D is already smaller than D_c.

These conclusions can be tested by using the numerical solutions described in Section 3 and Fig. 2. The total heat transfer rate removed from the $H \times L$ stack is $q' = nq''L$. The overall thermal conductance $q'/(T_{max}-T_\infty)$ can be nondimensionalized by using the q'_{max} scale recognized in equation (30)

$$B_2 = \frac{q'}{\dot{m}'c_P(T_{max}-T_\infty)}. \quad (34)$$

The relationship between B_2 and the nondimensional parameters of the numerical solution is

$$B_2 = \left[\left(\frac{D}{L}+\frac{t}{L}\right)M\theta_{max}\,Pr\right]^{-1} \quad (35)$$

where M is the nondimensional mass flowrate recommended by the right-hand side of equation (33)

$$M = \frac{\dot{m}'L}{\mu H}. \quad (36)$$

In terms of M, equation (33) states that D_c/L is of the order of $Pr^{-2/3}M^{-1/2}$, which is why the group $(D/L)Pr^{2/3}M^{1/2}$ is used now on the abscissae of Figs. 4(a) and (b). The two graphs were drawn for $M = 127$ and 63, which in the reference air case of Table 1 correspond to $Re = 1000$ and, respectively, $Re = 500$.

The numerical results confirm the validity of equation (33), because the transition between the high conductance limit of equation (30) and the decaying conductance of equation (32) is marked by an abscissa group of order 1. In conclusion, the stack operates in the high thermal conductance regime if, in an order of magnitude sense

$$\frac{D}{L}Pr^{2/3}M^{1/2} < 1. \quad (37)$$

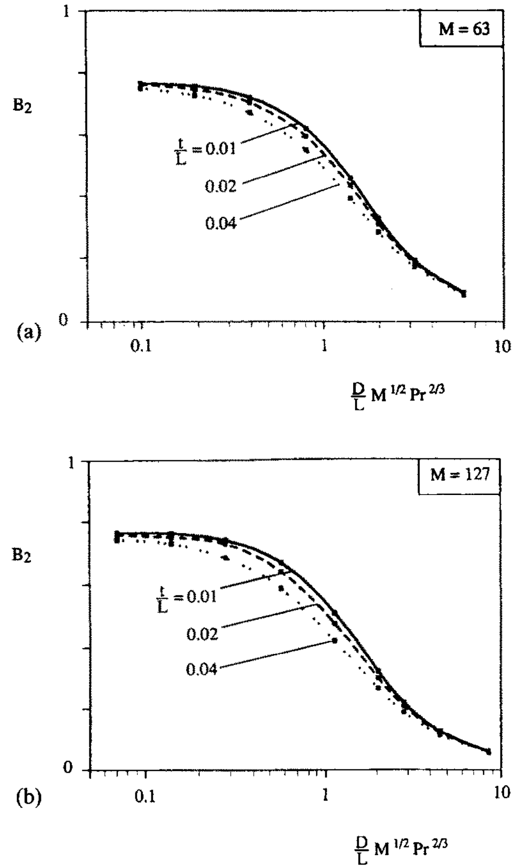

FIG. 4. The maximization of the overall thermal conductance when the mass flow rate is prescribed ($Pr = 0.7$).

When the abscissa group $(D/L)\,Pr^{2/3}M^{1/2}$ becomes of order 0.1 or less, the overall conductance B_2 approaches its highest (plateau) value, which is approximately 0.76. In other words, equation (34) becomes $q' \cong 0.76\dot{m}'c_P(T_{max}-T_\infty)$. This limiting value is somewhat lower than in the theoretical limit, equation (30), because in the theory the board surface was modelled as isothermal. In the numerical experiments of Figs. 4(a) and (b) the heat flux was assumed uniform, and T_{max} is the temperature at the trailing edge of the board.

6. OPTIMAL GEOMETRY OF PACKAGES WITH FIXED PUMPING POWER

Neither the constant-ΔP model nor the constant-$\dot{m}'$ model is appropriate when an H-thick package is the only item that is cooled by the stream created by the fan or pump. The lone package controls the resistance to the flow of the coolant, and both ΔP and $\dot{m}'$ vary as the package geometry changes. What remains constant in this case is the electric power input to the fan or pump, or the pumping power

$$\mathbf{P} = \frac{1}{\rho}\dot{m}'\Delta P. \quad (38)$$

(a) In the limit $D/L \rightarrow 0$ the flow through each D

channel is of the Poiseuille type, equation (2). If we combine equation (38) with the mass conservation statement $\dot{m}' = \rho UnD$ and equations (1) and (2), we obtain the mean velocity through each channel

$$U = \left[\frac{\mathbf{P}D(D+t)}{12\mu HL}\right]^{1/2}. \quad (39)$$

This can be substituted into equation (30), in which $\dot{m}' = \rho UnD$, to obtain

$$q'_a = \rho c_P D(T_w - T_\infty)\left[\frac{\mathbf{P}H}{12\mu L(1+t/D)}\right]^{1/2}. \quad (40)$$

In conclusion, when the board-to-board spacing is sufficiently small, the total heat transfer rate decreases almost proportionally with D.

(b) When the channel spacing is large enough so that the boundary layers are distinct the velocity in the channel is given by equation (5), or, after using equation (38) and $\dot{m}' = \rho U_\infty nD$

$$\frac{U_\infty L}{\nu} = \left(\frac{\mathbf{P}L^2(D+t)}{1.328\mu\nu^2 H}\right)^{2/5}. \quad (41)$$

The total heat transfer rate is $q'_b = 2nq'_1$, which can be developed further by using equations (1), (6) and (41)

$$q'_b = 1.254k(T_w - T_\infty)\, Pr^{1/3}\left(\frac{H}{D+t}\right)^{4/5}\left(\frac{\mathbf{P}L^2}{\mu\nu^2}\right)^{1/5}. \quad (42)$$

In the boundary layer limit, the total heat transfer rate decreases almost as $D^{-4/5}$ as the board-to-board spacing increases. The maximum q' corresponds to an optimal D value of the same order as the one obtained by intersecting the asymptotes (40) and (42)

$$\frac{D_{opt}}{L} \cong 2.26 Pr^{-10/27}\left[\frac{\mathbf{P}L^3(1+t/D_{opt})}{\mu\nu^2 H}\right]^{-1/6}. \quad (43)$$

We learn in this way that the optimal board-to-board spacing is almost insensitive to changes in the specified pumping power $\mathbf{P}$ and board thickness t. How large a D_{opt} value is recommended by equation (43) can be seen after noting that equation (41) can be rewritten as

$$\frac{U_\infty L}{\nu} \sim \left[\frac{\mathbf{P}L^3(1+t/D)}{\mu\nu^2 H}\right]^{1/3} Pr^{-4/27}. \quad (44)$$

In this equation, the numerical factor of order 1 has been neglected. The boundary layer regime scaling law (44) applies in an order of magnitude sense even at the $q'_a \sim q'_b$ intersection, which is represented by equation (43). Therefore if we eliminate the $\mathbf{P}$ group between equations (43) and (44), we find that

$$\frac{D_{opt}}{L} \sim \left(\frac{U_\infty L}{\nu}\right)^{-1/2} Pr^{-4/9}. \quad (45)$$

If $Pr \sim 1$ and the flow is laminar approaching transition, $U_\infty L/\nu \sim 10^4$, equation (45) shows that D_{opt} must be of the order of one-hundredth of the board length. The optimal spacing increases as the Reynolds number $U_\infty L/\nu$ decreases.

The scale of the maximum total heat transfer rate that corresponds to the optimal spacing D_{opt}, is obtained by substituting equation (43) into either equation (40) or equation (42)

$$q'_{max} \lesssim 0.65k(T_w - T_\infty)\frac{H}{L} Pr^{17/27}\Phi^{1/3}\left(1+\frac{t}{D_{opt}}\right)^{-2/3}. \quad (46)$$

The number Φ is the nondimensional pumping power defined as

$$\Phi = \frac{\mathbf{P}L^3}{\mu\nu^2 H} \quad (47)$$

which means that according to equation (43) the optimal D/L ratio is of the order of $Pr^{-10/27}[\Phi(1+t/D_{opt})]^{-1/6}$. This observation is the basis for choosing the abscissa parameter used in Fig. 5. In conclusion, the maximum heat transfer rate is proportional to the pumping power raised to the power 1/3.

The numerical solutions described in Section 3 and Fig. 2 can be used to test the validity of the optimization results developed in this section. The overall thermal conductance of a package with only one side of the board heated is $q'/(T_{max} - T_\infty)$, where $q' = nq''L$. The nondimensional conductance is defined by using the scale derived in equation (46)

$$B_3 = \frac{q'/(T_{max} - T_\infty)}{k(H/L)\, Pr^{17/27}\Phi^{1/3}}. \quad (48)$$

The relationship between B_3 and the dimensionless parameters of the numerical solution (D/L, Φ, t/L, Pr) is provided by

$$B_3 = \left[\left(\frac{D}{L} + \frac{t}{L}\right)\Phi^{1/3}\theta_{max} Pr^{17/27}\right]^{-1}. \quad (49)$$

The numerical results of Figs. 5(a)–(c) confirm the validity of the optimal spacing prediction made in equation (43). This conclusion can be summarized by using the group shown on the abscissa

$$\frac{D_{opt}}{L}\left(1+\frac{t}{D_{opt}}\right)^{1/6} Pr^{10/27}\Phi^{1/6} \cong 2.1 \quad (50)$$

which reproduces equation (43) almost exactly. Three Φ values were used in the numerical simulations: 1.35×10^4, 3.2×10^4 and 5.9×10^4. These correspond to the Re values of 500, 750 and 1000 in the reference case mentioned in Table 1, in which the coolant is air. The 2.1 constant that emerges on the right-hand side of equation (50) appears to be insensitive to changes in Φ and t/L.

The peak values of the thermal conductance curves can be correlated by noting that equation (46) can be rewritten as

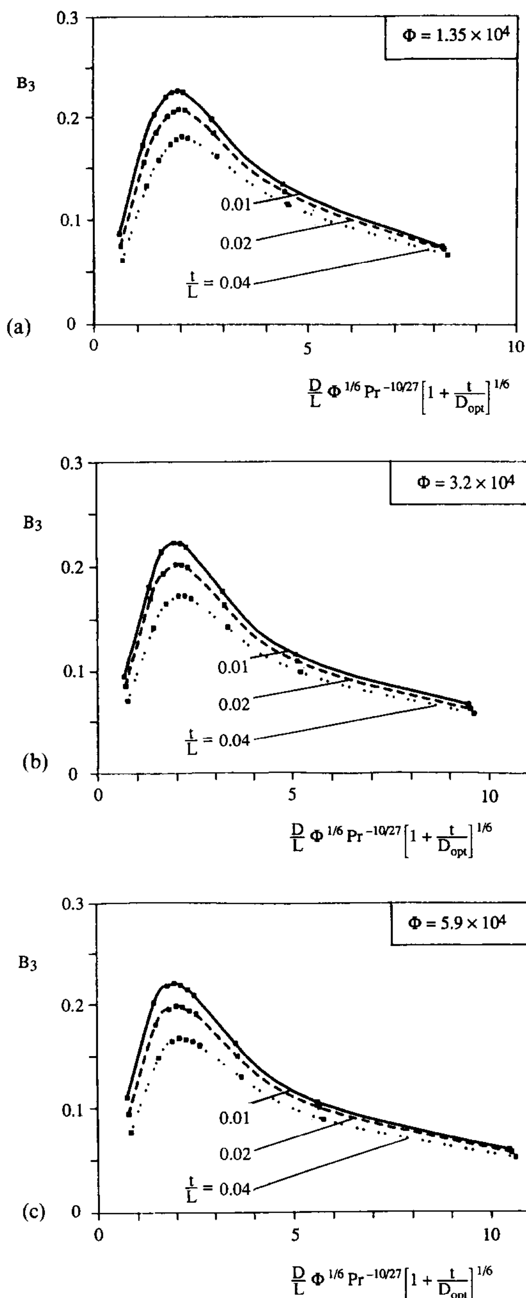

FIG. 5. The maximization of the overall thermal conductance when the pumping power is prescribed ($Pr = 0.7$).

$$B_{3,\mathrm{peak}} \leqslant \frac{0.65}{1+\frac{1}{C_3}\frac{t}{L}Pr^{10/27}\Phi^{1/6}\left(1+\frac{t}{D_{\mathrm{opt}}}\right)^{1/6}} \tag{51}$$

in which $C_3 = 2.1$ is the empirical constant identified in equation (50). The $B_{3,\mathrm{peak}}$ data are correlated within 10% by the simpler expression

$$B_{3,\mathrm{peak}} \cong \frac{0.21}{1+\frac{1}{2.1}\frac{t}{L}Pr^{10/27}\Phi^{1/6}}. \tag{52}$$

This expression is simpler than equation (51) because the group $(1+t/D_{\mathrm{opt}})^{1/6}$ is approximately equal to 1 in all the numerical cases that are being correlated. Note finally that equation (52) confirms also the direction of the inequality sign in equation (51).

7. CONCLUSIONS

In this paper, we have developed a series of theoretical results for estimating the optimal spacing of heat generating boards in a stack cooled by single-phase laminar forced convection. These results were validated by numerical simulations of the complete flow and heat transfer phenomenon. Three different design problems were considered, according to how the stack is mounted in the greater flow circuitry of the electrical apparatus. The main conclusions of this study are:

(a) *Fixed pressure drop.* The optimal board-to-board spacing is independent of the board thickness, and is given by the nondimensional correlation of equation (27). The maximum overall thermal conductance that corresponds to $D = D_{\mathrm{opt}}$ is summarized in nondimensional form in equation (29).

(b) *Fixed mass flowrate.* The overall thermal conductance of the stack reaches the highest level indicated by equation (30) when the board-to-board spacing D is less than the critical spacing D_c indicated by equation (33). The same conclusion is stated in nondimensional terms by equation (37).

(c) *Fixed pumping power.* The optimal board-to-board spacing is given by equation (50), and the corresponding peak value of the overall thermal conductance of the stack is correlated by equation (52).

Acknowledgements—Adrian Bejan's work was supported by the IBM Corporation, Research Triangle Park, North Carolina. Stefano Mereu and Enrico Sciubba received a grant for CPU-time on the IBM-3090/VF-600 of the Consortium for Intensive Computational Applications (CASPUR) at the University of Rome 1.

REFERENCES

1. F. P. Incropera, Convection heat transfer in electronic equipment cooling, *J. Heat Transfer* **110,** 1097–1111 (1988).
2. G. P. Peterson and A. Ortega, Thermal control of electronic equipment and devices, *Adv. Heat Transfer* **20,** 181–314 (1990).
3. A. Bejan, *Convection Heat Transfer*, Chapter 4, Problem 11. Wiley, New York (1984).
4. A. Bar-Cohen and W. M. Rohsenow, Thermally optimum spacing of vertical, natural convection cooled, parallel plates, *J. Heat Transfer* **106,** 116–123 (1984).
5. W. Elenbaas, Heat dissipation of parallel plates by free convection, *Physica* **9,** 1–23 (1942).
6. E. K. Levy, Optimum plate spacing for laminar natural convection heat transfer from parallel vertical isothermal flat plates, *J. Heat Transfer* **93,** 463–465 (1971).

7. S. H. Kim, N. K. Anand and L. S. Fletcher, Free convection between series of vertical parallel plates with embedded line heat sources, *J. Heat Transfer* **113,** 108–115 (1991).
8. N. K. Anand, S. H. Kim and L. S. Fletcher, The effect of plate spacing on free convection between heated parallel plates, ASME **HTD 153,** 81–87 (1990).
9. N. K. Anand, S. H. Kim and L. S. Fletcher, The effect of plate spacing on free convection between heated parallel plates, *J. Heat Transfer* **114,** 515–518 (1992).
10. R. C. Schmidt and S. V. Patankar, A numerical study of laminar forced convection across heated rectangular blocks in two-dimensional ducts, ASME Paper No. 86-WA/HT-88 (1986).
11. J. Davalath and Y. Bayazitoglu, Forced convection cooling across rectangular blocks, *J. Heat Transfer* **109,** 321–328 (1987).
12. D. B. Tuckerman and R. F. W. Pease, High-performance heat sinking for VLSI, *IEEE Electron Dev. Letts*, **EDL-2,** 126–129 (1981).
13. R. W. Knight, J. S. Goodling and D. J. Hall, Optimal thermal design of forced convection heat sinks—analytical, *J. Electr. Packaging* **113,** 313–321 (1991).
14. A. Bejan and E. Sciubba, The optimal spacing of parallel plates cooled by forced convection, *Int. J. Heat Mass Transfer* **35,** 3259–3264 (1992).
15. A. Bejan, *Heat Transfer*, p. 328. Wiley, New York (1993).
16. *FIDAP Theoretical Manual.* Fluid Dynamics International, Evanston, IL, V. 6.03 (1991).